



Automated quantitative evaluation of fetal atrioventricular annular plane systolic excursion

L. HERLING^{1,2}, J. JOHNSON^{1,2}, K. FERM-WIDLUND², A. ZAMPRAKOU^{1,3}, M. WESTGREN^{1,2#} and G. ACHARYA^{1,2,4#}

¹Department of Clinical Science, Intervention and Technology - CLINTEC, Karolinska Institutet, Stockholm, Sweden; ²Center for Fetal Medicine, Department of Obstetrics and Gynecology, Karolinska University Hospital, Stockholm, Sweden; ³Pregnancy and Delivery Medical Unit, Department of Obstetrics and Gynecology, Karolinska University Hospital, Stockholm, Sweden; ⁴Women's Health and Perinatology Research Group, Department of Clinical Medicine, UiT-The Arctic University of Norway, Tromsø, Norway

KEYWORDS: annular plane systolic excursion; atrioventricular plane displacement; automated analysis; fetal cardiac function; fetal echocardiography; M-mode; tissue Doppler imaging

CONTRIBUTION

What are the novel findings of this work?

Fetal atrioventricular plane displacement in the left and right ventricular walls and interventricular septum of the fetal heart (i.e. mitral, tricuspid and septal annular plane systolic excursion, respectively) can be analyzed automatically over several cardiac cycles using myocardial velocity traces obtained by color tissue Doppler imaging (cTDI).

What are the clinical implications of this work?

Automated analysis of cTDI cine-loops of the four-chamber view of the fetal heart has the potential to simplify assessment of fetal atrioventricular plane displacement, enabling gathering of larger amounts of data. Such data could potentially be used in machine-learning models to facilitate prenatal assessment of different fetal disease states and evaluation of fetal risk at an individual level.

ABSTRACT

Objectives The primary aim of this study was to evaluate the feasibility of automated measurement of fetal atrioventricular (AV) plane displacement (AVPD) over several cardiac cycles using myocardial velocity traces obtained by color tissue Doppler imaging (cTDI). The secondary objectives were to establish reference ranges for AVPD during the second half of normal pregnancy, to assess fetal AVPD in prolonged pregnancy in relation to adverse perinatal outcome and to evaluate AVPD in

fetuses with a suspicion of intrauterine growth restriction (IUGR).

Methods The population used to develop the reference ranges consisted of women with an uncomplicated singleton pregnancy at 18–42 weeks of gestation (n = 201). The prolonged-pregnancy group comprised women with an uncomplicated singleton pregnancy at $\geq 41 + 0$ weeks of gestation (n = 107). The third study cohort comprised women with a singleton pregnancy and suspicion of IUGR, defined as an estimated fetal weight < 2.5th centile or an estimated fetal weight < 10th centile and umbilical artery pulsatility index > 97.5th centile (n = 35). Cine-loops of the four-chamber view of the fetal heart were recorded using cTDI. Regions of interest were placed at the AV plane in the left and right ventricular walls and the interventricular septum, and myocardial velocity traces were integrated and analyzed using an automated algorithm developed in-house to obtain mitral (MAPSE), tricuspid (TAPSE) and septal (SAPSE) annular plane systolic excursion. Gestational-age specific reference ranges were constructed and normalized for cardiac size. The correlation between AVPD measurements obtained using cTDI and those obtained by anatomic M-mode were evaluated, and agreement between these two methods was assessed using Bland–Altman analysis. The mean Z-scores of fetal AVPD in the cohort of prolonged pregnancies were compared between cases with normal and those with adverse outcome using Mann–Whitney U-test. The mean Z-scores of fetal AVPD in IUGR fetuses were compared with those in the normal reference population using Mann–Whitney U-test. Inter- and intraobserver

Correspondence to: Dr L. Herling, Center for Fetal Medicine, Department of Obstetrics and Gynecology, Karolinska University Hospital, Stockholm, Sweden, and CLINTEC, Karolinska Institutet, Stockholm, Sweden (e-mail: lotta.herling@ki.se)

#M.W. and G.A. contributed equally to this study.

Accepted: 21 May 2021

variability for acquisition of cTDI recordings and offline analysis was assessed by calculating coefficients of variation (CV) using the root mean square method.

Results Fetal MAPSE, SAPSE and TAPSE increased with gestational age but did not change significantly when normalized for cardiac size. The fitted mean was highest for TAPSE throughout the second half of gestation, followed by SAPSE and MAPSE. There was a significant correlation between MAPSE ($r = 0.64$; $P < 0.001$), SAPSE ($r = 0.72$; $P < 0.001$) and TAPSE ($r = 0.84$; $P < 0.001$) measurements obtained by M-mode and those obtained by cTDI. The geometric means of ratios between AVPD measured by cTDI and by M-mode were 1.38 (95% limits of agreement (LoA), 0.84–2.25) for MAPSE, 1.00 (95% LoA, 0.72–1.40) for SAPSE and 1.20 (95% LoA, 0.92–1.57) for TAPSE. In the prolonged-pregnancy group, the mean \pm SD Z-scores for MAPSE (0.14 ± 0.97), SAPSE (0.09 ± 1.02) and TAPSE (0.15 ± 0.90) did not show any significant difference compared to the reference ranges. Twenty-one of the 107 (19.6%) prolonged pregnancies had adverse perinatal outcome. The AVPD Z-scores were not significantly different between pregnancies with normal and those with adverse outcome in the prolonged-pregnancy cohort. The mean \pm SD Z-scores for SAPSE (-0.62 ± 1.07 ; $P = 0.006$) and TAPSE (-0.60 ± 0.89 ; $P = 0.002$) were significantly lower in the IUGR group compared to those in the normal reference population, but the differences were not significant when the values were corrected for cardiac size. The interobserver CVs for the automated measurement of MAPSE, SAPSE and TAPSE were 28.1%, 17.7% and 15.3%, respectively, and the respective intraobserver CVs were 33.5%, 15.0% and 17.9%.

Conclusions This study showed that fetal AVPD can be measured automatically by integrating cTDI velocities over several cardiac cycles. Automated analysis of AVPD could potentially help gather larger datasets to facilitate use of machine-learning models to study fetal cardiac function. The gestational-age associated increase in AVPD is most likely a result of increasing cardiac size, as the AVPD normalized for cardiac size did not change significantly between 18 and 42 weeks. A decrease was seen in TAPSE and SAPSE in IUGR fetuses, but not after correction for cardiac size. © 2021 The Authors. *Ultrasound in Obstetrics & Gynecology* published by John Wiley & Sons Ltd on behalf of International Society of Ultrasound in Obstetrics and Gynecology.

INTRODUCTION

Atrioventricular (AV) plane displacement (AVPD), often expressed as mitral annular plane systolic excursion (MAPSE), septal annular plane systolic excursion (SAPSE) and tricuspid annular plane systolic excursion (TAPSE), is a major contributor to cardiac pumping^{1,2} and a measure of longitudinal cardiac function. AVPD is defined as the distance between the two positions where the AV plane is the farthest from the apex and closest to the apex

during a cardiac cycle³. In healthy adults, examined using magnetic resonance imaging, AVPD accounts for 80% of the right-ventricular (RV) and 60% of the left-ventricular (LV) stroke volume⁴. Even in situations in which the absolute AVPD is decreased, the longitudinal contribution remains the main component of LV stroke volume^{5,6}. Longitudinal cardiac function, which is executed by longitudinal myocardial fibers, is considered to be the first affected in the event of hypoxia^{7,8}.

In fetuses, AVPD can be evaluated using ultrasound techniques, such as M-mode, tissue Doppler imaging (TDI) and speckle tracking^{3,9}. AVPD depends on body¹⁰ and cardiac¹¹ size, and absolute values increase with gestational age (GA)¹².

Using color TDI (cTDI), AVPD can be analyzed by integrating myocardial velocities. Through the application of an in-house automated algorithm, which has been used previously to analyze myocardial velocities and cardiac cycle time intervals in fetuses^{13,14}, automated measurements from several cardiac cycles can be obtained. Such an analysis allows for a quicker evaluation of large amounts of data that could potentially help in evaluating AVPD as a tool to detect cardiac dysfunction in fetuses with different disease states.

The primary aim of this study was to evaluate the feasibility of automated measurement of AVPD over several cardiac cycles from cTDI cine-loops of the four-chamber view of the fetal heart. A comparison of cTDI-derived AVPD with AVPD measured using anatomic M-mode was also performed. The secondary objectives were, first, to establish reference ranges for AVPD during the second half of normal pregnancy, second, to assess AVPD in prolonged pregnancy in relation to adverse perinatal outcome and, third, to assess AVPD in fetuses with suspicion of intrauterine growth restriction (IUGR).

METHODS

This was a cross-sectional study conducted at the Center for Fetal Medicine, Karolinska University Hospital, Stockholm, Sweden, between September 2009 and February 2017. Ethical approval was obtained from the Stockholm Regional Ethics Committee (DNr 2009/1617-31/2, 2012/895-31/4 and 2017/539-32). All women gave written informed consent to participate.

The first cohort, used for the development of reference ranges for AVPD in the second half of pregnancy, consisted of women with an uncomplicated singleton pregnancy between 18 and 42 weeks of gestation ($n = 201$). Exclusion criteria were conception after *in-vitro* fertilization/intracytoplasmic sperm injection treatment, maternal complications at inclusion, such as pre-eclampsia, chronic hypertension or diabetes, and fetal chromosomal or major structural abnormalities discovered during pregnancy or postnatally. Pregnancies were dated by measuring the biparietal diameter in the second trimester¹⁵. Each fetus was included only once. Reference ranges for myocardial velocities and cardiac

cycle time intervals based on the same population have been published previously¹⁴.

The second cohort, used to assess AVPD in prolonged pregnancy in relation to adverse perinatal outcome, comprised women with an uncomplicated pregnancy who attended a routine appointment at $\geq 41+0$ weeks of gestation ($n=107$) and underwent an ultrasound examination between $41+0$ and $41+5$ weeks. A composite adverse perinatal outcome was defined as the presence of at least one of the following: intrapartum fetal scalp blood lactate >4.8 mmol/L, umbilical cord arterial pH <7.15 , 5-min Apgar score <7 or 5-min Apgar score for muscle tone <2 . Data regarding the feasibility of automated analysis of fetal myocardial velocity measurements obtained by cTDI have been published previously using this cohort¹⁶.

The third cohort included, as part of a pilot study, women with a singleton fetus with a suspicion of IUGR, defined as an estimated fetal weight (EFW) $<2.5^{\text{th}}$ centile or an EFW $<10^{\text{th}}$ centile and umbilical artery pulsatility index $>97.5^{\text{th}}$ centile. The definition used is based on Swedish reference ranges for estimation of fetal weight and umbilical artery cut-off values^{17,18}.

Fetal echocardiography using cTDI was performed by an experienced ultrasonographer (K.F.-W.) using a GE Vivid-i ultrasound imaging system, equipped with a 3S-RS 1.9–3.8-MHz phased-array transducer (GE Vingmed, Horten, Norway) or a Vivid S6 ultrasound imaging system with a M4S-RS 1.9–4.1-MHz phased-array transducer (GE CV Ultrasound, Haifa, Israel). An apical or basal four-chamber view of the fetal heart was acquired and cine-loops of consecutive cardiac cycles were recorded using cTDI. The insonation angle was kept as close as possible to the long axis of the heart (and always $<30^\circ$) and the image was adjusted to obtain as high a frame rate as possible. Offline analysis was performed using EchoPAC version 201 (GE Vingmed). The region of interest (ROI) was adjusted in height and width according to GA, as in previous research¹³, and placed at the AV plane in the LV and RV walls and the interventricular septum (IVS). All ROIs were placed by one operator (L.H.). Myocardial velocity traces were subsequently exported from EchoPAC to MATLAB (R2019b; MathWorks, Natick, MA, USA) and then analyzed using an automated software tool developed in-house. Cardiac cycle time intervals were defined by the software. The program in MATLAB, i.e. the automated analysis described, has several user-defined functions and some MATLAB built-in functions^{2,19}. The myocardial velocity data were integrated and AVPD was obtained automatically and defined as the maximum distance covered by the AV plane during the cardiac cycle (Figure 1). AVPD in the LV, IVS and RV were called MAPSE, SAPSE and TAPSE, respectively, and according to nomenclature used previously in fetuses. The analysis is a fully automated procedure and no manual marking of the traces is needed once the velocity traces are exported to MATLAB. The average of all available cardiac cycles was also calculated.

The fetal cardiac size was measured as the longitudinal diameter (apex to base) in early systole, right after the closure of the AV valves in diastole. Calipers were placed from the midpoint of the atria at the outer border to the outer border of the apex. The cardiac size, i.e. the longitudinal diameter of the heart²⁰, was used to normalize AVPD measurements.

In a subset of 30 fetuses from the first cohort (i.e. the cohort used for development of the reference ranges), AVPD was measured additionally using anatomic M-mode echocardiography for comparison with the cTDI-derived AVPD measurements obtained using the automated technique. The M-mode cursor was placed through the lateral leaflets of the AV valves and the IVS to obtain an alignment with the IVS $<30^\circ$. The total AVPD was measured according to previously described

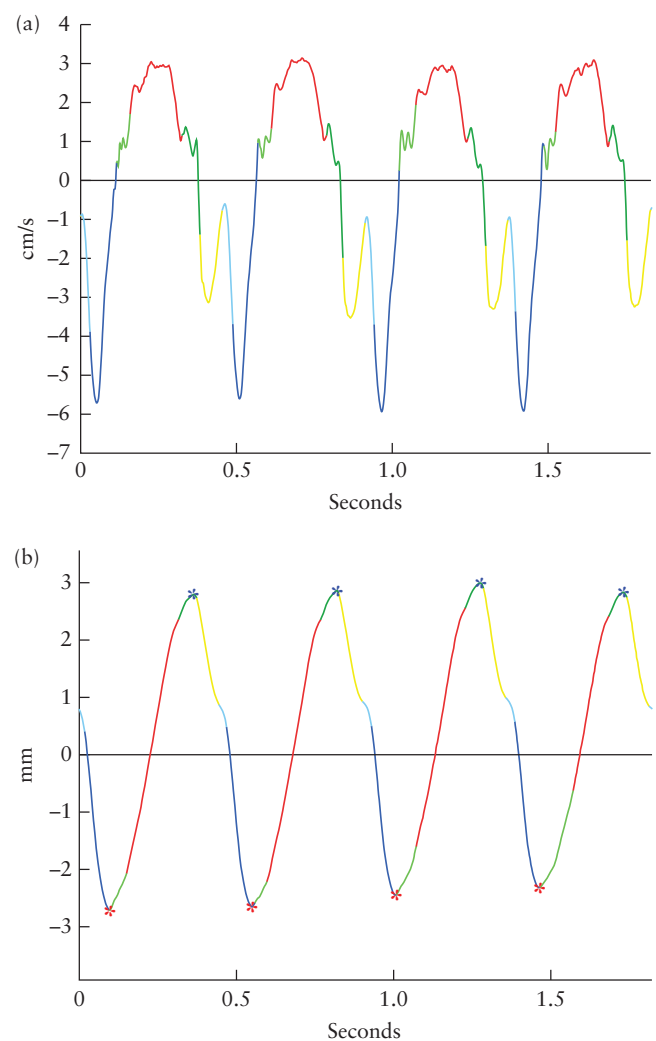


Figure 1 Automated analysis of a myocardial velocity trace from the right ventricular wall (a) and a trace showing the tricuspid annular peak systolic excursion (TAPSE) (b), obtained by color tissue Doppler imaging in a normal 34-week fetus. The colors indicate the different phases in the cardiac cycle, as defined by the automated algorithm: atrial contraction (■), pre-ejection (■), ventricular ejection (■), post-ejection (■), rapid ventricular filling (■), slow ventricular filling (■). The blue and red asterisks in (b) indicate the maximum amplitude of TAPSE.

techniques^{21,22}. The average of three measurements was calculated.

The inter- and intraobserver variability of the acquisition of cTDI recordings and offline analysis was evaluated using a Vivid S6 ultrasound imaging system with a M4S-RS 1.9–4.1-MHz phased-array transducer (GE CV Ultrasound). The interobserver variability was evaluated by two ultrasonographers (K.F.-W. and L.H.) who examined 25 fetuses, between 19 and 41 weeks of gestation, between December 2016 and February 2017. Subsequently, 22 of these fetuses were examined again by the first ultrasonographer (K.F.-W.) approximately 10 min later, and the intraobserver variability for the entire procedure was evaluated by comparing the two recordings. This means that the calculated coefficients of variation (CV) also reflect the variability associated with the change in fetal physiological state and position, as well as the resulting technical challenges during the examination period, not just the operator-related measurement variability. ROIs were placed by one operator (L.H.) and all generated myocardial velocity traces were analyzed by the automated algorithm.

Statistical analysis

Data analysis was performed using IBM SPSS Statistics for Windows, version 25.0 (IBM Corp., Armonk, NY, USA) and MATLAB (MathWorks). Continuous variables are presented as mean \pm SD or median (interquartile range), as appropriate. Categorical variables are presented as n (%). The statistical approach described by Royston and Wright²³ was used to create reference intervals for MAPSE, SAPSE and TAPSE. Box–Cox power transformation was used to decide the appropriate type of transformation. The best-fitting fractional polynomials were chosen from a list of 44 regression models based on R^2 value, using NCSS 2020 Statistical Software (NCSS LLC, Kaysville, UT, USA) to construct mean curves of each dependent variable in relation to GA, expressed in exact weeks (decimal days). The normality of the distribution of the Z-scores was checked using the Shapiro–Wilk test. Mean, SD and CI curves as a function of GA were calculated and plotted. The equations of the polynomial regression were used to calculate the estimated mean, 5th and 95th centiles for the corresponding GA as fitted mean \pm 1.645 SD. CIs were calculated for the fitted mean, 5th and 95th centiles. The same procedure was then performed for values normalized for cardiac size.

The MAPSE, SAPSE and TAPSE of the prolonged pregnancies with an adverse neonatal outcome were plotted on the reference ranges of the normal population. The mean Z-scores of AVPD in the cohort of prolonged pregnancies were compared between cases with a normal outcome and those with an adverse outcome using Mann–Whitney *U*-test.

The AVPD measurements in the IUGR cohort were plotted on the graphs of the reference ranges and the mean Z-scores of AVPD were compared between the IUGR

group and the normal population using Mann–Whitney *U*-test.

The correlation between AVPD measurements obtained using cTDI and those obtained by anatomic M-mode was evaluated using Spearman's correlation, and agreement between the two measurement methods was tested for bias and precision using Bland–Altman analysis of log-transformed data^{24–26}. We defined precision by the 95% limits of agreement (LoA) (± 1.96 SD) and bias as the difference between the geometric mean of all individual ratios between pairs of values obtained using the two methods and the line of equality. The statistical significance level was set to $P < 0.05$. To assess intra- and interobserver variability, CVs were calculated using the root mean square method²⁷.

RESULTS

Baseline characteristics, ultrasound data and pregnancy outcomes of the normal group ($n = 201$), prolonged pregnancies ($n = 107$) and fetuses with a suspicion of IUGR ($n = 35$) are presented in Table 1.

Normal reference ranges for cTDI-derived AVPD

Initially, 202 pregnant women were enrolled in this cohort. After the exclusion of one woman whose fetus was diagnosed with muscular ventricular septal defect and bicuspid aortic valve, the cohort consisted of 201 women. In total, 603 fetal myocardial velocity traces (201 each from LV, IVS and RV) were available for analysis and subsequent integration to obtain AVPD data. One RV trace was excluded due to severe artifacts and two IVS traces could not be analyzed. The mean \pm SD number of cardiac cycles analyzed were 10.2 ± 2.6 in the LV, 10.3 ± 2.7 in the IVS and 10.3 ± 2.6 in the RV.

The interobserver CVs for the automated measurement of AVPD on cTDI cine loop recordings of the four-chamber view of the fetal heart obtained consecutively by two sonographers in 25 fetuses were 28.1%, 17.7% and 15.3% for MAPSE, SAPSE and TAPSE, respectively. The intraobserver CVs for the automated measurement of AVPD on cine loop recordings obtained by a single sonographer approximately 10 min apart in 22 fetuses were 33.5%, 15.0% and 17.9% for MAPSE, SAPSE and TAPSE, respectively. The measurement variability of automated analysis on the same cine loop recording was zero on repeated evaluation.

The best model for all variables was a quadratic polynomial fit. MAPSE was transformed logarithmically, whereas SAPSE and TAPSE did not require any transformation. MAPSE, SAPSE and TAPSE all increased with GA (Figure 2 and Tables 2–4). The regression equations are displayed in Table 5. The fitted mean was highest in TAPSE throughout the second half of gestation, followed by SAPSE and MAPSE. Reference ranges with the corresponding 95% CIs calculated for the fitted mean and 5th and 95th centiles are displayed in Figure 2. A Z-score and centile calculator for MAPSE, SAPSE and

TAPSE obtained by cTDI and analyzed automatically is provided in Appendix S1.

When corrected for cardiac size, all three variables showed a weak non-significant trend to decline from 18 weeks of gestation onwards. Reference ranges corrected for cardiac size with the corresponding 95% CIs calculated for the fitted mean, 5th and 95th centiles are displayed in Figure 3.

Comparison between AVPD measurements obtained in the same fetus by cTDI and anatomic M-mode was performed in 30 pregnancies from the reference population. The fetuses evaluated by anatomic M-mode were distributed evenly across gestation, with five fetuses included in each of the following GA windows: 18 + 0 to 21 + 6, 22 + 0 to 25 + 6, 26 + 0 to 29 + 6, 30 + 0 to 33 + 6, 34 + 0 to 37 + 6 and 38 + 0 to 42 + 6 weeks. We observed a statistically significant correlation between MAPSE ($r = 0.64$; $P < 0.001$), SAPSE ($r = 0.72$; $P < 0.001$) and TAPSE ($r = 0.84$; $P < 0.001$) measurements obtained by M-mode and those obtained by cTDI (Figure 4). When 30 pairs of log-transformed AVPD measurements were tested using Bland–Altman analysis, the geometric means of ratios between AVPD measured by cTDI and M-mode were 1.38 (95% LoA, 0.84–2.25) for MAPSE, 1.00 (95% LoA, 0.72–1.40) for SAPSE and 1.20 (95% LoA, 0.92–1.57) for TAPSE (Figure 5).

Prolonged pregnancy and adverse outcome

A total of 107 women were included in this cohort and 321 myocardial velocity traces were analyzed. The mean \pm SD number of cardiac cycles analyzed were 8.5 ± 1.3 in the LV, 8.9 ± 0.9 in the IVS and 8.6 ± 0.7 in the RV. The mean \pm SD Z-scores for MAPSE (0.14 ± 0.97), SAPSE (0.09 ± 1.02) and TAPSE (0.15 ± 0.90) in this cohort did not show any significant difference compared to the reference ranges of the normal population ($P > 0.05$) (Figure 2). No significant differences were found when the measurements were corrected for cardiac size. Twenty-one of the 107 (19.6%) neonates had an adverse perinatal outcome. No significant differences in AVPD Z-scores were found between the pregnancies with normal and those with adverse outcome within the prolonged-pregnancy cohort.

Fetuses with suspicion of IUGR

A total of 35 fetuses with a suspicion of IUGR were included and 105 velocity traces were analyzed and integrated to obtain AVPD data. The mean \pm SD number of cardiac cycles analyzed were 9.0 ± 2.8 in the LV, 9.4 ± 2.5 in the IVS and 10.3 ± 1.6 in the RV. The mean \pm SD Z-scores for SAPSE (-0.62 ± 1.07 ;

Table 1 Maternal baseline characteristics, ultrasound data and pregnancy outcome in 201 normal pregnancies between 18 and 42 weeks' gestation, 107 pregnancies at ≥ 41 weeks' gestation and 35 pregnancies with a suspicion of intrauterine growth restriction (IUGR)

Variable	Normal cohort (n = 201)	Prolonged pregnancy (n = 107)	Suspected IUGR (n = 35)
Maternal data			
Age (years)	30.1 \pm 5.2	31.0 \pm 5.2	30.8 \pm 5.3
BMI (kg/m ²)	23.7 \pm 3.9	24.9 \pm 5.2	25.1 \pm 5.5
Spontaneous pregnancy	201 (100)	100 (93.5)	31 (88.6)
Nulliparous	81 (40.3)	45 (42.1)	17 (48.6)
Smoker	12 (6.0)	2 (1.9)	6 (17.1)
Ultrasound data			
GA at scan/inclusion (weeks)	30.4 \pm 7.2	41.1 \pm 0.2	33.2 \pm 3.4
UA-PI > 97.5 th centile	0 (0)	4 (3.7)	14 (40.0)
Apical position of fetal heart	107 (53.2)	32 (29.9)	14 (40.0)
Frame rate	208.3 \pm 6.8	206.3 \pm 15.5	208.1 \pm 10.4
Pregnancy outcome*			
Pre-eclampsia	4 (2.0)	0 (0)	11 (31.4)
GA at delivery (weeks)	40.0 \pm 1.4	41.7 \pm 0.4	35.6 \pm 3.8
Post-term delivery $\geq 42 + 0$ weeks	19 (9.6)	35 (32.7)	0 (0)
Preterm delivery < 37 weeks	4 (2.0)	0 (0)	19 (54.3)
Mode of delivery			
Normal vaginal	147 (74.2)	85 (79.4)	18 (51.4)
Vacuum extraction	22 (11.1)	9 (8.4)	0 (0)
Cesarean section	29 (14.6)	13 (12.1)	17 (48.6)
Elective	NA	3 (2.8)	1 (2.9)
Emergency	NA	10 (9.3)	16 (45.7)
Birth weight (g)	3576 \pm 501	3840 \pm 423	1973 \pm 632
Female neonate	96 (48.5)	55 (51.4)	21 (60.0)
Cord arterial pH \ddagger	7.25 \pm 0.09	7.22 \pm 0.09	7.29 \pm 0.09
Cord venous pH \ddagger	7.32 \pm 0.07	7.31 \pm 0.07	7.38 \pm 0.06
5-min Apgar score < 7	0 (0)	1 (0.9)	2 (5.7)

Data are given as mean \pm SD or *n* (%). *Pregnancy outcome data were missing for three women in the control group who delivered in other hospitals. Data available for: †138, 83 and 21 cases in the normal, prolonged-pregnancy and IUGR cohorts, respectively; ‡49, 98 and six cases in the normal, prolonged-pregnancy and IUGR cohorts, respectively. BMI, body mass index; GA, gestational age; NA, not available; PI, pulsatility index; UA, umbilical artery.

$P=0.006$) and TAPSE (-0.60 ± 0.89 ; $P=0.002$) were significantly lower in the IUGR group in comparison to the reference ranges of the normal population (mean Z-scores were zero for SAPSE, MAPSE and TAPSE) (Figure 2). The mean \pm SD Z-score for MAPSE was -0.13 ± 0.67 ($P=0.160$). When corrected for cardiac size, there were no significant differences in the mean Z-scores for SAPSE, TAPSE and MAPSE between the normal population and the IUGR group.

DISCUSSION

This study showed that automated measurement of AVPD in the LV, IVS and RV over several cardiac cycles from cTDI cineloops is feasible in the second half of pregnancy. The measurements at all three locations, i.e. MAPSE, SAPSE and TAPSE, increased with gestation; however, when corrected for cardiac size, all three variables showed a weak non-significant trend to decline from 18 weeks of gestation onwards. We observed a significant correlation

between AVPD measurements obtained by M-mode and those obtained by cTDI. The AVPD measured by automated analysis of cTDI cineloops was similar to that measured by M-mode for SAPSE (had least bias), 20% lower for TAPSE and 38% lower for MAPSE with varied precision. In the group with a suspicion of IUGR, SAPSE and TAPSE Z-scores were significantly lower compared to the reference ranges, but these differences did not remain significant when data were normalized for cardiac size.

An increase in MAPSE, SAPSE and TAPSE throughout gestation has been shown previously using both anatomic and conventional M-mode^{12,21,22,28}. Previous studies using M-mode^{12,22} demonstrated the highest values in the RV wall and the lowest values in the IVS, which is in contrast to our finding of the lowest values being in the LV wall. The reason for this difference is unclear and might result from positioning of the ROI in the IVS to avoid disturbances from the valves or shadowing of the LV wall when a back-up apical four-chamber view is obtained.

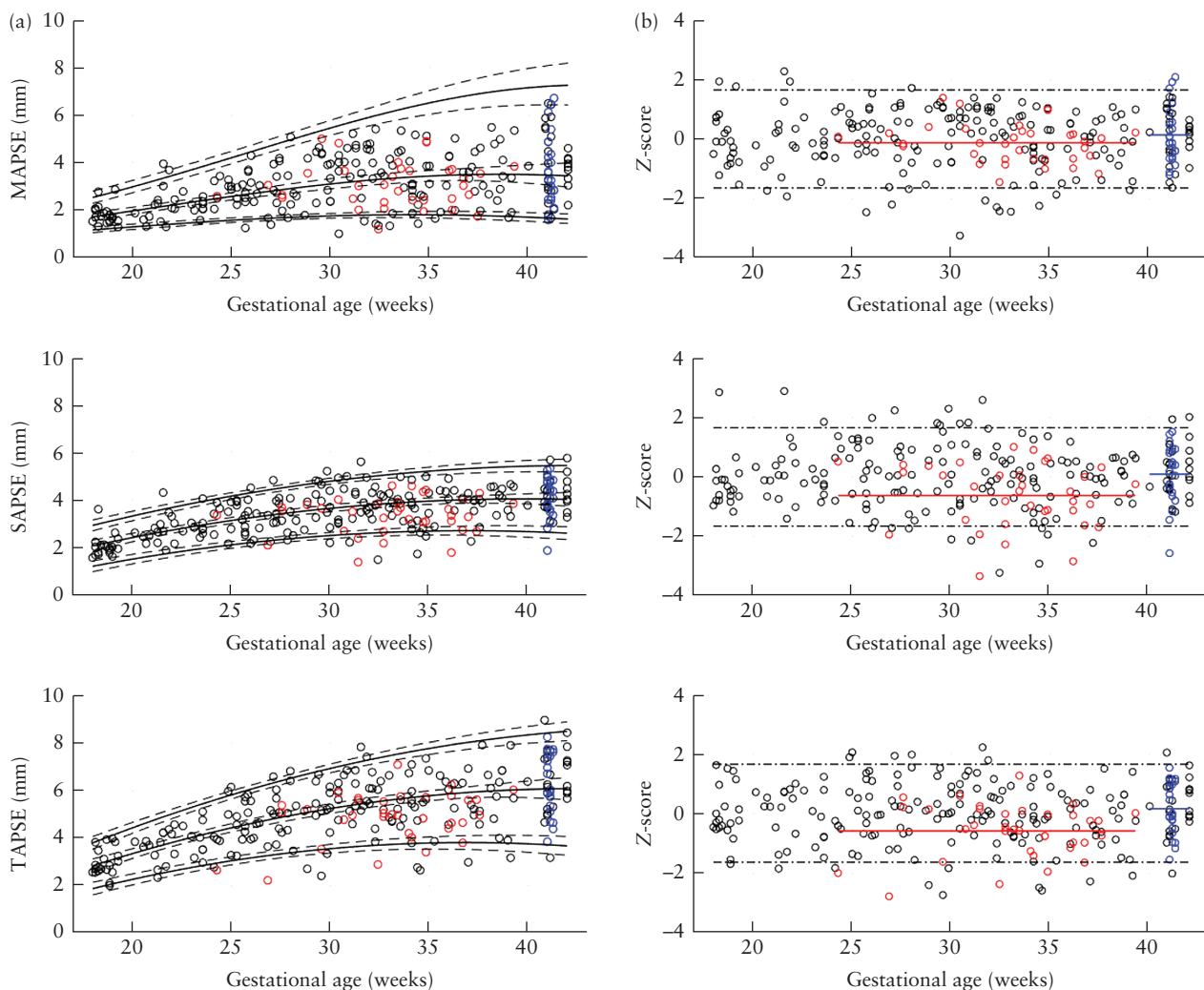


Figure 2 (a) Scatterplots of mitral annular plane systolic excursion (MAPSE), septal annular plane systolic excursion (SAPSE) and tricuspid annular plane systolic excursion (TAPSE) obtained by color tissue Doppler imaging and analyzed automatically, in 201 low-risk pregnancies (○), 35 fetuses with a suspicion of intrauterine growth restriction (IUGR) (○) and 21 fetuses at $\geq 41 + 0$ weeks of gestation that had an adverse outcome (○), plotted against gestational age. The fitted mean and 5th and 95th centiles, with corresponding 95% CIs (---), of the low-risk cohort are shown. (b) Corresponding Z-scores for MAPSE, SAPSE and TAPSE. —, mean in fetuses with suspicion of IUGR; —, mean in prolonged pregnancies with adverse outcome. ----, ± 1.645 SD.

Table 2 Measurements of fetal mitral annular plane systolic excursion (in mm), obtained by color tissue Doppler imaging and analyzed automatically, according to gestational age (GA)

GA (weeks)	n	Centile						
		2.5 th	5 th	10 th	50 th	90 th	95 th	97.5 th
18	15	1.11	1.19	1.29	1.74	2.34	2.55	2.74
19	5	1.16	1.25	1.37	1.86	2.53	2.76	2.98
20	4	1.22	1.31	1.44	1.98	2.73	2.99	3.23
21	8	1.27	1.38	1.51	2.11	2.93	3.22	3.50
22	4	1.32	1.43	1.58	2.23	3.14	3.46	3.77
23	8	1.37	1.49	1.65	2.35	3.35	3.71	4.05
24	6	1.41	1.54	1.71	2.47	3.57	3.96	4.33
25	12	1.45	1.59	1.77	2.59	3.78	4.21	4.62
26	6	1.49	1.64	1.83	2.71	4.00	4.47	4.91
27	11	1.52	1.68	1.88	2.82	4.21	4.72	5.21
28	6	1.55	1.72	1.93	2.92	4.42	4.97	5.50
29	8	1.58	1.75	1.97	3.02	4.63	5.22	5.79
30	10	1.60	1.78	2.01	3.11	4.82	5.46	6.08
31	10	1.61	1.80	2.04	3.20	5.01	5.69	6.36
32	9	1.62	1.81	2.07	3.28	5.19	5.92	6.63
33	8	1.62	1.82	2.08	3.34	5.36	6.13	6.88
34	13	1.62	1.83	2.09	3.40	5.52	6.33	7.13
35	5	1.61	1.82	2.10	3.45	5.66	6.51	7.36
36	5	1.60	1.81	2.10	3.48	5.78	6.68	7.57
37	8	1.58	1.80	2.09	3.51	5.89	6.83	7.76
38	8	1.56	1.78	2.07	3.52	5.98	6.96	7.93
39	4	1.53	1.75	2.05	3.52	6.06	7.06	8.07
40	4	1.50	1.72	2.02	3.51	6.11	7.15	8.19
41	15	1.47	1.69	1.98	3.49	6.14	7.21	8.29
42	9	1.43	1.64	1.94	3.45	6.16	7.25	8.36

Table 3 Measurements of fetal septal annular plane systolic excursion (in mm), obtained by color tissue Doppler imaging and analyzed automatically, according to gestational age (GA)

GA (weeks)	n	Centile						
		2.5 th	5 th	10 th	50 th	90 th	95 th	97.5 th
18	15	1.09	1.26	1.44	2.10	2.77	2.95	3.12
19	5	1.24	1.41	1.60	2.28	2.96	3.15	3.32
20	4	1.38	1.55	1.75	2.45	3.14	3.34	3.51
21	8	1.51	1.68	1.89	2.60	3.32	3.52	3.70
22	4	1.63	1.81	2.02	2.75	3.49	3.69	3.88
23	8	1.75	1.93	2.14	2.90	3.65	3.86	4.04
24	6	1.85	2.04	2.26	3.03	3.80	4.02	4.21
25	12	1.95	2.14	2.37	3.15	3.94	4.17	4.36
26	6	2.04	2.24	2.47	3.27	4.08	4.31	4.50
27	11	2.12	2.32	2.56	3.38	4.20	4.44	4.64
28	6	2.19	2.40	2.64	3.48	4.32	4.56	4.77
29	8	2.26	2.47	2.71	3.57	4.43	4.68	4.89
30	10	2.32	2.53	2.78	3.66	4.54	4.79	5.00
31	9	2.36	2.58	2.84	3.74	4.63	4.89	5.11
32	9	2.41	2.63	2.89	3.80	4.72	4.98	5.20
33	8	2.44	2.67	2.93	3.86	4.80	5.06	5.29
34	13	2.46	2.70	2.96	3.92	4.87	5.14	5.37
35	5	2.48	2.72	2.99	3.96	4.93	5.20	5.44
36	5	2.49	2.73	3.01	3.99	4.98	5.26	5.50
37	8	2.49	2.73	3.02	4.02	5.03	5.31	5.56
38	7	2.48	2.73	3.02	4.04	5.06	5.35	5.61
39	4	2.46	2.72	3.01	4.05	5.09	5.39	5.64
40	4	2.43	2.70	3.00	4.05	5.11	5.41	5.67
41	15	2.40	2.67	2.97	4.05	5.13	5.43	5.70
42	9	2.36	2.63	2.94	4.04	5.13	5.44	5.71

MAPSE, SAPSE and TAPSE showed a weak non-significant trend to decline from 18 weeks of gestation when corrected for cardiac size. It is well-known that myocardial velocities and, consequently, displacement data depend on the size of the heart²⁹. Our results indicate that cardiac size largely explains the increase in AVPD measurement seen throughout gestation. Fetal size and different measurements of the heart such as the longitudinal diameter of the heart and heart area^{11,28} have been suggested to normalize AVPD. In this study, we chose to normalize the data using the longitudinal diameter of the heart, as this measurement was the most stable to perform in the four-chamber view acquired and has been used previously by other authors¹¹.

In the group of fetuses with a suspicion of IUGR, mean TAPSE and SAPSE were significantly lower compared to the normal group. However, this difference did not remain significant when measurements were corrected for cardiac size, suggesting that the smaller AVPD measurements are related to the smaller heart of IUGR fetuses. This is in analogy with the fact that IUGR fetuses are suggested to maintain cardiac output in spite of alterations in hemodynamic afterload due to placental insufficiency and hypoxemia^{30,31}. Nevertheless, conclusions should be interpreted with caution, as the small number of patients with suspected IUGR and the broad inclusion criteria could have influenced the results. Furthermore, when correcting for cardiac size using the longitudinal

Table 4 Measurements of fetal tricuspid annular plane systolic excursion (in mm), obtained by color tissue Doppler imaging and analyzed automatically, according to gestational age (GA)

GA (weeks)	n	Centile						
		2.5 th	5 th	10 th	50 th	90 th	95 th	97.5 th
18	15	1.70	1.88	2.09	2.84	3.59	3.80	3.98
19	5	1.88	2.08	2.30	3.10	3.90	4.12	4.32
20	4	2.06	2.27	2.51	3.35	4.19	4.43	4.64
21	8	2.23	2.45	2.70	3.59	4.48	4.73	4.95
22	4	2.38	2.61	2.88	3.81	4.75	5.02	5.25
23	8	2.53	2.77	3.05	4.03	5.01	5.29	5.53
24	6	2.66	2.91	3.21	4.24	5.27	5.56	5.81
25	12	2.78	3.05	3.35	4.43	5.51	5.81	6.08
26	6	2.90	3.17	3.49	4.61	5.74	6.06	6.33
27	11	3.00	3.28	3.62	4.79	5.96	6.29	6.58
28	6	3.09	3.39	3.73	4.95	6.17	6.51	6.81
29	8	3.17	3.48	3.84	5.10	6.37	6.72	7.03
30	10	3.24	3.56	3.93	5.24	6.55	6.92	7.25
31	10	3.29	3.63	4.01	5.37	6.73	7.11	7.45
32	9	3.34	3.69	4.08	5.49	6.90	7.29	7.64
33	8	3.38	3.73	4.14	5.60	7.05	7.46	7.82
34	13	3.40	3.77	4.20	5.69	7.19	7.62	7.99
35	4	3.42	3.80	4.23	5.78	7.33	7.77	8.15
36	5	3.42	3.81	4.26	5.86	7.45	7.90	8.29
37	8	3.41	3.82	4.28	5.92	7.56	8.03	8.43
38	8	3.39	3.81	4.29	5.98	7.66	8.14	8.56
39	4	3.37	3.79	4.28	6.02	7.75	8.24	8.67
40	4	3.33	3.76	4.27	6.05	7.83	8.34	8.77
41	15	3.28	3.73	4.24	6.07	7.90	8.42	8.87
42	9	3.21	3.68	4.21	6.08	7.96	8.49	8.95

Table 5 Regression equations for MAPSE, SAPSE and TAPSE obtained by color tissue Doppler imaging and analyzed automatically

Variable	n	Fitted equation	a	b	c	SE (of b)	SE (of c)	P (of b)	P (of c)	Adjusted R ²
Mean (mm)										
MAPSE	201	$\log(y) = a + bGA + cGA^2$	-0.5281	0.0557	-0.000727	0.012	0.0002	< 0.001	< 0.001	0.339
SAPSE	199	$y = a + bGA + cGA^2$	-2.4385	0.3260	-0.0041	0.060	0.0010	< 0.001	< 0.001	0.450
TAPSE	200	$y = a + bGA + cGA^2$	-3.6869	0.4601	-0.0054	0.082	0.0014	< 0.001	< 0.001	0.551
SD										
MAPSE	201	$a + bGA$	0.0290	0.0040	—	0.001	—	< 0.001	—	0.062
SAPSE	199	$a + bGA$	0.2618	0.0141	—	0.005	—	0.0098	—	0.029
TAPSE	200	$a + bGA$	-0.0753	0.0366	—	0.007	—	< 0.001	—	0.108

a, intercept; b, slope/coefficient; c, coefficient; GA, gestational age; MAPSE, mitral annular plane systolic excursion; SAPSE, septal annular plane systolic excursion; SE, standard error; TAPSE, tricuspid annular plane systolic excursion.

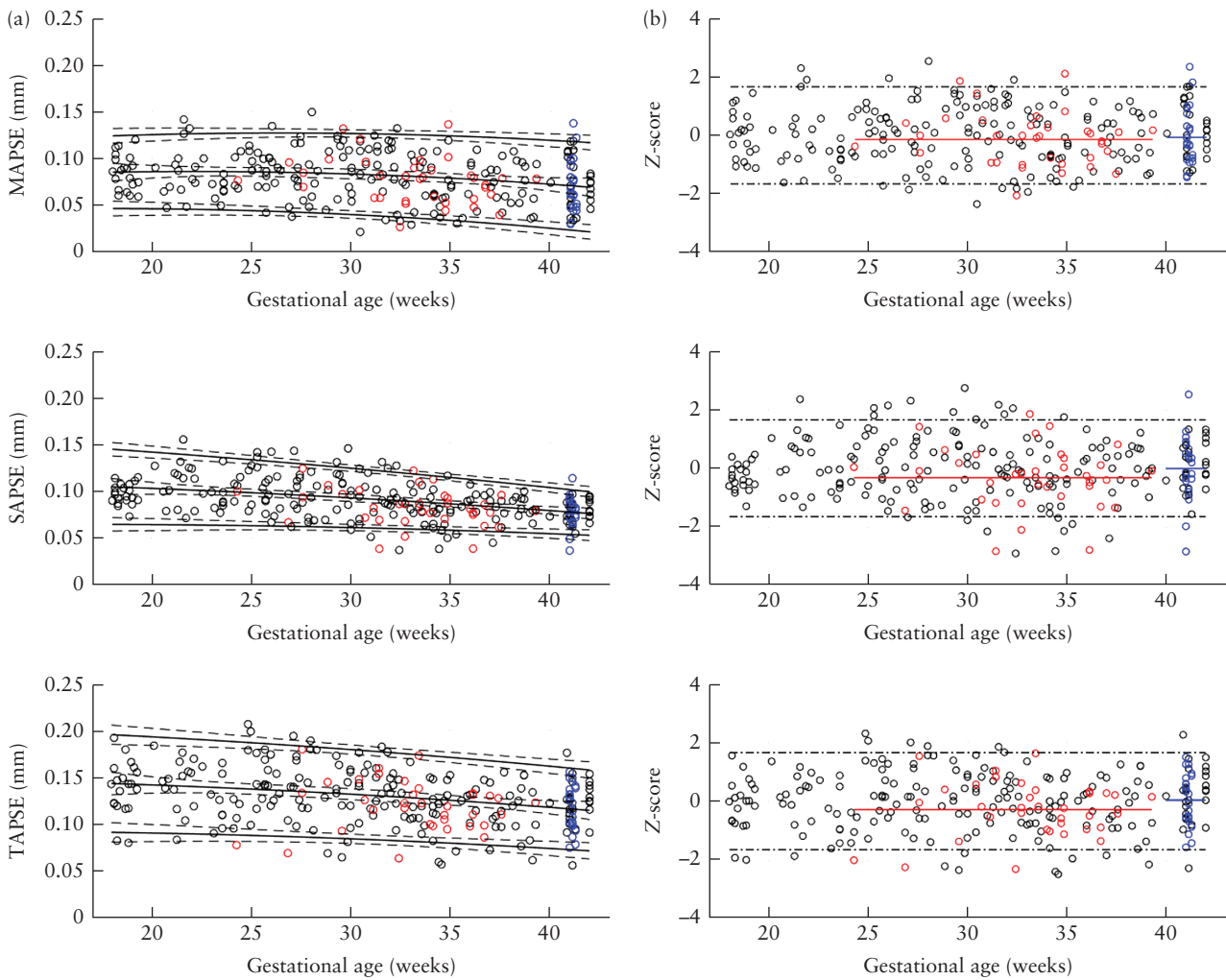


Figure 3 (a) Scatterplots of mitral annular plane systolic excursion (MAPSE), septal annular plane systolic excursion (SAPSE) and tricuspid annular plane systolic excursion (TAPSE) obtained by color tissue Doppler imaging and analyzed automatically, with values corrected for measurement of cardiac size, in 201 low-risk pregnancies (○), 35 fetuses with a suspicion of intrauterine growth restriction (IUGR) (○) and 21 fetuses at ≥ 41 + 0 weeks of gestation that had an adverse outcome (○), plotted against gestational age. The fitted mean and 5th and 95th centiles, with corresponding 95% CIs (---), of the low-risk cohort are shown. (b) Corresponding Z-scores for MAPSE, SAPSE and TAPSE. —, mean in fetuses with suspicion of IUGR; —, mean in prolonged pregnancies with adverse outcome. ----, ± 1.645 SD.

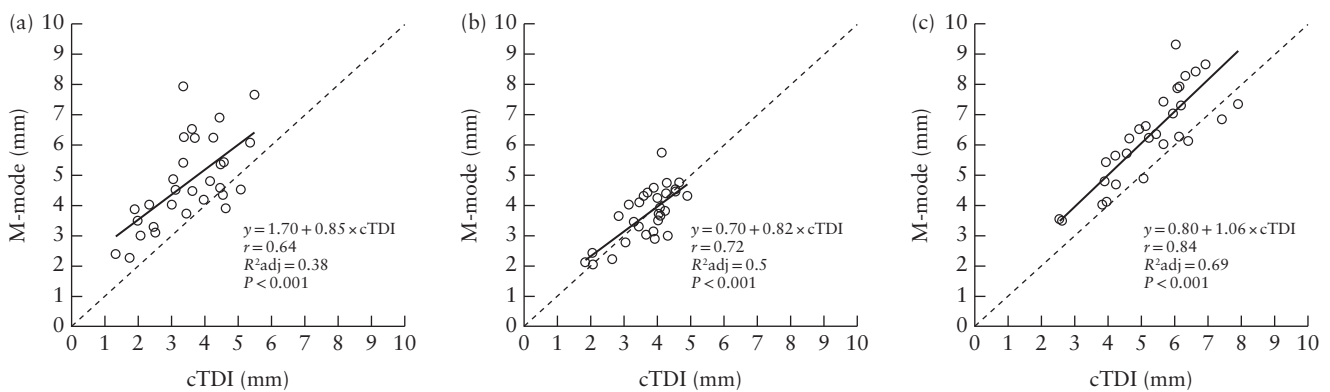


Figure 4 Comparison of measurements of mitral annular plane systolic excursion (a), septal annular plane systolic excursion (b) and tricuspid annular plane systolic excursion (c) obtained by color tissue Doppler imaging (cTDI) and those obtained by anatomic M-mode, in 30 low-risk fetuses at 18 + 0 to 42 + 6 weeks' gestation. The dashed line represents the line of equality. R²adj, adjusted R² value.

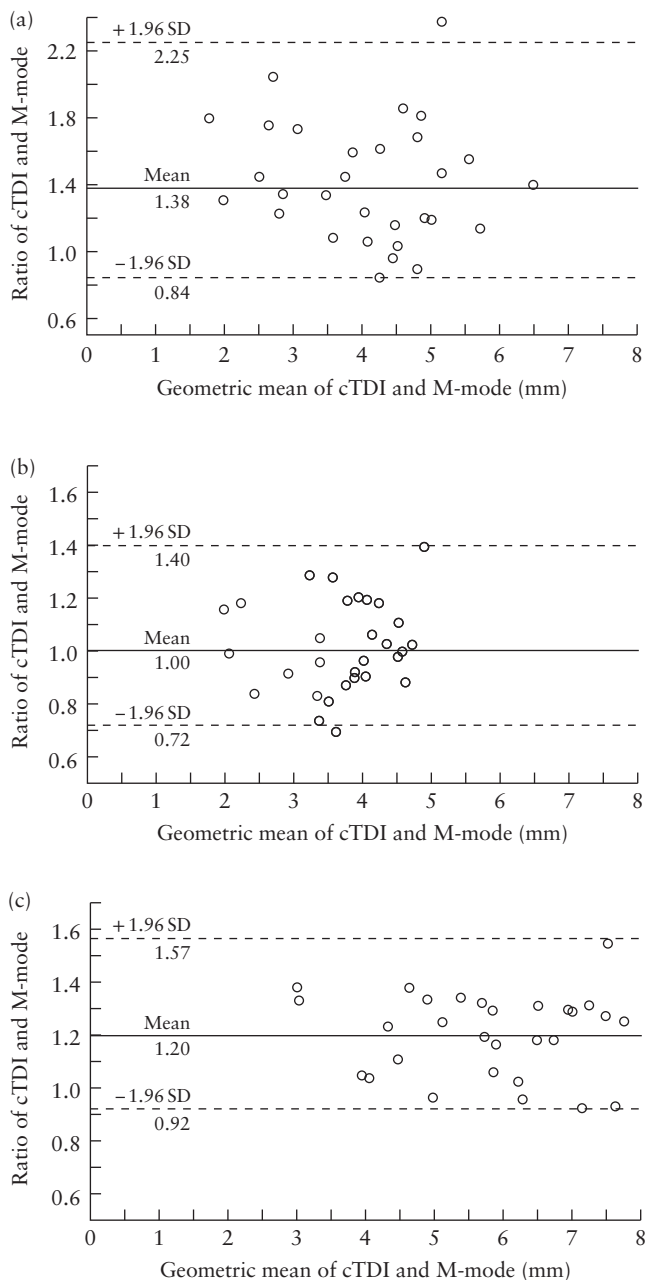


Figure 5 Bland–Altman plots demonstrating agreement between measurements of mitral annular plane systolic excursion (a), septal annular plane systolic excursion (b) and tricuspid annular plane systolic excursion (c) obtained by color tissue Doppler imaging (cTDI) and by anatomic M-mode in 30 low-risk fetuses at 18 + 0 to 42 + 6 weeks' gestation. Solid line represents mean and dashed upper and lower lines represent mean \pm 1.96 SD (95% limits of agreement).

diameter of the heart, the width of the heart is not considered. This might also have influenced results, as both IUGR fetuses at term and fetuses with an estimated weight $< 10^{\text{th}}$ centile with normal umbilical artery blood flow have shown a more globular ventricular geometry with an increased width of the heart^{30,32}. Nevertheless, Cruz-Lemini *et al.*¹¹ showed a decrease in MAPSE, SAPSE and TAPSE measured by M-mode, after correction for the longitudinal diameter of the heart, in IUGR fetuses compared with normal controls.

M-mode overestimates AVPD in cases of angle deviation, as opposed to cTDI which underestimates the velocity and, thus, the AVPD, with increasing angle of deviation. This is illustrated in this study by SAPSE (which has the smallest angle of insonation being centrally located), which showed similar values when evaluated by cTDI and M-mode. MAPSE and TAPSE, which have increasing angles of insonation, demonstrated higher M-mode compared to cTDI measurements.

Inter- and intraobserver CVs ranged from 15.3% to 33.5%, with TAPSE and SAPSE showing lower and MAPSE showing higher values. This is partly in line with the findings reported by Peixoto *et al.*²², who showed poor-to-moderate intra- and interobserver agreement when assessing AVPD using M-mode. The authors also repeated the actual ultrasound examination in a similar manner as we did in this study and, consequently, the variability also reflected changes in fetal physiological state and position as well as the resulting technical challenges during the examination period, not only the operator-related measurement variability. As expected, repeat automated analysis of the same velocity recordings always gave the same results with no measurement variability.

A strength of this study is that the automated algorithm simplifies the analysis of cTDI traces by evaluating several cardiac cycles. As opposed to M-mode analysis, this technique also provides an automated measurement from a defined point in a well-defined curve, which is likely to diminish the subjectivity of measurements. It is also possible to assess what part of the movement of the AV plane occurs during different cardiac phases. Moreover, there is no variability from the point when the traces have been obtained, as the automated algorithm performs identically on every occasion. The variability would come from factors such as the variability of the examination itself, including intrinsic cardiac variability, angle dependency when measuring velocities, the manual positioning of ROIs and fetal movements.

Limitations of this study are the small number of patients in the IUGR cohort and that only the longitudinal diameter of the heart was used to normalize measurements.

In conclusion, MAPSE, SAPSE and TAPSE, evaluating longitudinal function in the fetal heart, could be measured using an automated algorithm. All three variables showed an increase with GA, but no significant change was observed when corrected for cardiac size. A decrease was seen in TAPSE and SAPSE in IUGR fetuses compared with the normal population, but not after correction for cardiac size. Comparison of AVPD measurements obtained by the automated cTDI technique with those measured by M-mode echocardiography showed similar values for SAPSE, but relatively greater differences for TAPSE and MAPSE due to the inherent technical aspects related to both methods. Our results need to be evaluated further in a larger cohort of patients in which the automated method could potentially help in

gathering larger amount of data to assist in the use of machine-learning/deep-learning models.

ACKNOWLEDGMENTS

The authors thank all women who participated in the study and all colleagues at Karolinska University Hospital, Stockholm, Sweden, involved in their care.

REFERENCES

- Carlsson M, Ugander M, Mosen H, Buhre T, Arheden H. Atrioventricular plane displacement is the major contributor to left ventricular pumping in healthy adults, athletes, and patients with dilated cardiomyopathy. *Am J Physiol Heart Circ Physiol* 2007; **292**: H1452–1459.
- Lundback S. Cardiac pumping and function of the ventricular septum. *Acta Physiol Scand Suppl* 1986; **550**: 1–101.
- Acharya G. Measurement of atrioventricular annular plane displacement has been revived: will it prove to be useful in assessing fetal cardiac function? *Ultrasound Obstet Gynecol* 2013; **42**: 125–129.
- Carlsson M, Ugander M, Heiberg E, Arheden H. The quantitative relationship between longitudinal and radial function in left, right, and total heart pumping in humans. *Am J Physiol Heart Circ Physiol* 2007; **293**: H636–644.
- Asgeirsson D, Hedstrom E, Jogi J, Pahlm U, Steding-Ehrenborg K, Engblom H, Arheden H, Carlsson M. Longitudinal shortening remains the principal component of left ventricular pumping in patients with chronic myocardial infarction even when the absolute atrioventricular plane displacement is decreased. *BMC Cardiovasc Disord* 2017; **17**: 208.
- Pahlm U, Seemann F, Engblom H, Gyllenhammar T, Halvorsen S, Hansen HS, Erlinge D, Atar D, Heiberg E, Arheden H, Carlsson M. Longitudinal left ventricular function is globally depressed within a week of STEMI. *Clin Physiol Funct Imaging* 2018. DOI: 10.1111/cpf.12521.
- Henein MY, Priestley K, Davarashvili T, Buller N, Gibson DG. Early changes in left ventricular subendocardial function after successful coronary angioplasty. *Br Heart J* 1993; **69**: 501–506.
- Jones CJ, Raposo L, Gibson DG. Functional importance of the long axis dynamics of the human left ventricle. *Br Heart J* 1990; **63**: 215–220.
- Carvalho JS, O'Sullivan C, Shinebourne EA, Henein MY. Right and left ventricular long-axis function in the fetus using angular M-mode. *Ultrasound Obstet Gynecol* 2001; **18**: 619–622.
- Wandt B, Bojo L, Wranne B. Influence of body size and age on mitral ring motion. *Clin Physiol* 1997; **17**: 635–646.
- Cruz-Lemini M, Crispi F, Valenzuela-Alcaraz B, Figueras F, Sitges M, Gomez O, Bijns B, Gratacos E. Value of annular M-mode displacement vs tissue Doppler velocities to assess cardiac function in intrauterine growth restriction. *Ultrasound Obstet Gynecol* 2013; **42**: 175–181.
- Gardiner HM, Pasquini L, Wolfenden J, Barlow A, Li W, Kulinskaya E, Henein M. Myocardial tissue Doppler and long axis function in the fetal heart. *Int J Cardiol* 2006; **113**: 39–47.
- Herling L, Johnson J, Ferm-Widlund K, Lindgren P, Acharya G, Westgren M. Automated analysis of color tissue Doppler velocity recordings of the fetal myocardium using a new algorithm. *Cardiovasc Ultrasound* 2015; **13**: 39.
- Herling L, Johnson J, Ferm-Widlund K, Bergholm F, Elmstedt N, Lindgren P, Sonesson SE, Acharya G, Westgren M. Automated analysis of fetal cardiac function using color tissue Doppler imaging in second half of normal pregnancy. *Ultrasound Obstet Gynecol* 2019; **53**: 348–357.
- Saltvedt S, Almstrom H, Kublickas M, Reilly M, Valentin L, Grunewald C. Ultrasound dating at 12–14 or 15–20 weeks of gestation? A prospective cross-validation of established dating formulae in a population of *in-vitro* fertilized pregnancies randomized to early or late dating scan. *Ultrasound Obstet Gynecol* 2004; **24**: 42–50.
- Herling L, Johnson J, Ferm-Widlund K, Bergholm F, Lindgren P, Sonesson SE, Acharya G, Westgren M. Automated analysis of fetal cardiac function using color tissue Doppler imaging. *Ultrasound Obstet Gynecol* 2018; **52**: 599–608.
- Marsal K, Persson PH, Larsen T, Lilja H, Selbing A, Sultan B. Intrauterine growth curves based on ultrasonically estimated foetal weights. *Acta Paediatr* 1996; **85**: 843–848.
- Arstrom K, Eliasson A, Hareide JH, Marsal K. Fetal blood velocity waveforms in normal pregnancies. A longitudinal study. *Acta Obstet Gynecol Scand* 1989; **68**: 171–178.
- Bergholm F. En algoritim för att finna maxima och minima i “periodisk” kolvliknande rörelse. KTH Technology and Health: Stockholm, Sweden, 2016.
- Garcia-Otero L, Gomez O, Rodriguez-Lopez M, Torres X, Soveral I, Sepulveda-Martinez A, Guirado L, Valenzuela-Alcaraz B, Lopez M, Martinez JM, Gratacos E, Crispi F. Nomograms of Fetal Cardiac Dimensions at 18–41 Weeks of Gestation. *Fetal Diagn Ther* 2020; **47**: 387–398.
- Lee-Tannock A, Hay K, Gooi A, Kumar S. Longitudinal Reference Ranges for Tricuspid Annular Plane Systolic Excursion and Mitral Annular Plane Systolic Excursion in Normally Grown Fetuses. *J Ultrasound Med* 2020; **39**: 929–937.
- Peixoto AB, Bravo-Valenzuela NJ, Martins WP, Tonni G, Mattar R, Moron AF, Pares DB, Araujo Júnior E. Reference ranges for the fetal mitral, tricuspid, and interventricular septum annular plane systolic excursions (mitral annular plane systolic excursion, tricuspid annular plane systolic excursion, and septum annular plane systolic excursion) between 20 and 36+6 weeks of gestation. *J Perinat Med* 2020; **48**: 601–608.
- Royston P, Wright EM. How to construct ‘normal ranges’ for fetal variables. *Ultrasound Obstet Gynecol* 1998; **11**: 30–38.
- Bland JM, Altman DG. Statistical methods for assessing agreement between two methods of clinical measurement. *Lancet* 1986; **1**: 307–310.
- Bland JM, Altman DG. Measuring agreement in method comparison studies. *Stat Methods Med Res* 1999; **8**: 135–160.
- Acharya G, Sitras V, Erkinaro T, Makikallio K, Kavasmaa T, Pakkila M, Huhta JC, Rasanen J. Experimental validation of uterine artery volume blood flow measurement by Doppler ultrasonography in pregnant sheep. *Ultrasound Obstet Gynecol* 2007; **29**: 401–406.
- Hyslop NP, White WH. Estimating precision using duplicate measurements. *J Air Waste Manag Assoc* 2009; **59**: 1032–1039.
- Mao YK, Zhao BW, Wang B. Z-Score Reference Ranges for Angular M-Mode Displacement at 22–40 Weeks’ Gestation. *Fetal Diagn Ther* 2017; **41**: 115–126.
- Batterham A, Shave R, Oxborough D, Whyte G, George K. Longitudinal plane colour tissue-Doppler myocardial velocities and their association with left ventricular length, volume, and mass in humans. *Eur J Echocardiogr* 2008; **9**: 542–546.
- Patey O, Carvalho JS, Thilaganathan B. Perinatal changes in cardiac geometry and function in growth-restricted fetuses at term. *Ultrasound Obstet Gynecol* 2019; **53**: 655–662.
- Kiserud T, Ebbing C, Kessler J, Rasmussen S. Fetal cardiac output, distribution to the placenta and impact of placental compromise. *Ultrasound Obstet Gynecol* 2006; **28**: 126–136.
- Hobbins JC, Gumina DL, Zaretsky MV, Driver C, Wilcox A, DeVore GR. Size and shape of the four-chamber view of the fetal heart in fetuses with an estimated fetal weight less than the tenth centile. *Am J Obstet Gynecol* 2019; **221**: 495.e1–9.

SUPPORTING INFORMATION ON THE INTERNET

The following supporting information may be found in the online version of this article:



Appendix S1 Z-score and centile calculator for mitral annular plane systolic excursion (MAPSE), septal annular plane systolic excursion (SAPSE) and tricuspid annular plane systolic excursion (TAPSE) obtained by color tissue Doppler imaging and analyzed automatically